Northumbria Research Link

Citation: Zhu, Jiangbo, Cai, Xinlun, Chen, Yujie and Yu, Siyuan (2013) Theoretical model for angular grating-based integrated optical vortex beam emitters. Optics Letters, 38 (8). p. 1343. ISSN 0146-9592

Published by: OSA

URL: https://doi.org/10.1364/OL.38.001343 <https://doi.org/10.1364/OL.38.001343>

This version was downloaded from Northumbria Research Link: http://nrl.northumbria.ac.uk/id/eprint/43290/

Northumbria University has developed Northumbria Research Link (NRL) to enable users to access the University's research output. Copyright © and moral rights for items on NRL are retained by the individual author(s) and/or other copyright owners. Single copies of full items can be reproduced, displayed or performed, and given to third parties in any format or medium for personal research or study, educational, or not-for-profit purposes without prior permission or charge, provided the authors, title and full bibliographic details are given, as well as a hyperlink and/or URL to the original metadata page. The content must not be changed in any way. Full items must not be sold commercially in any format or medium without formal permission of the copyright holder. The full policy is available online: http://nrl.northumbria.ac.uk/policies.html

This document may differ from the final, published version of the research and has been made available online in accordance with publisher policies. To read and/or cite from the published version of the research, please visit the publisher's website (a subscription may be required.)

Northumbria University NEWCASTLE

University Library

A theoretical model for angular grating-based integrated optical vortex beam emitters

Jiangbo Zhu,[1,*] Xinlun Cai,[2] Yujie Chen,[3] Siyuan Yu[2]

[1]*State Key Lab of ASIC & System, Department of Communication Science and Engineering, Fudan University, Shanghai, China*
[2]*Photonics Group, Merchant Venturers School of Engineering, University of Bristol, Bristol, UK.*
[3]*State Key Laboratory of Optoelectronic Materials and Technologies, Sun Yat-sen University, Guangzhou, China.*
**Corresponding author: zjb227@gmail.com*

Received Month X, XXXX; revised Month X, XXXX; accepted Month X,
XXXX; posted Month X, XXXX (Doc. ID XXXXX); published Month X, XXXX

We develop a theoretical model for the recently reported integrated optical vortex beam emitters that incorporate angular gratings in micro-ring resonators. Using azimuthally polarized dipole oscillators to represent emission scattered from the grating elements that are located along the inner wall of the ring waveguide, we obtain expressions for far-field components under the paraxial approximation. The results show that the emission is of the form of cylindrical vector Bessel beam with exactly defined optical orbital angular momentum, and can have azimuthal, radial, and longitudinal field components after propagation. The calculation results for field distributions in both near and far zone agree well with the experimental results.
© 2013 Optical Society of America
OCIS Codes: 050.1940, 050.4865, 230.3120.

Orbital angular momentum (OAM) is a degree of freedom of the photon in addition to polarization/spin. Unlike spin, OAM occupies an unbounded Hilbert space [1,2]. Classical manifestation of OAM is found in the azimuthally varying phase around the light beam axis leading to spiral wave fronts. Until recently, the manipulation of the OAM states of light has been restricted to complex and bulky optical components that are slow to respond, cumbersome to use, and with no clear route to scaling or integration [3,4]. A recent progress in OAM optics is the realization of integrated OAM beam emitters built on silicon platforms [5,6]. The principle of operation of the micron-sized OAM device in Ref. [6] is to extract light confined in the whispering gallery mode (WGM) of micro-ring resonator using a 2nd-order Bragg grating that scatters the WGM to a vertically emitted OAM mode. The device is capable of emitting optical beams with variable OAM states by detuning wavelength or by tuning the ring resonance. That is, for a micro-ring resonator with fixed number of grating elements, the OAM state of the emitted beam is only dependent on the wavelength. For quasi-transverse electric (TE) WGM with the dominant e-field component being E_r in the radial direction of the ring, the state of polarization (SOP) of the emitted near-field was found to be predominantly in the azimuthal (φ) direction. This stems from the position of the grating elements on the sidewall, where E_r is minimal but a strong E_φ exists. As the size of the grating element is very small (60 nm) compared to wavelength in the silicon waveguide (~650 nm for vacuum wavelength of 1550 nm), azimuthal polarized dipole radiation is a reasonable representation of the scattered field at each of the grating elements. In this Letter, this dipole-model is elaborated to give analytical expressions of the emitted field distribution. It is also demonstrated that the SOP of the vortex beams emitted is vectorial in nature, and a beam with topological charge of l is a linear combination of left and right circular polarized waves of charges $l-1$ and $l+1$ respectively.

Given the axial symmetry of the angular grating distribution, we establish the model in a normalized cylindrical coordinate (ρ, φ, ζ), in which ρ and ζ are the polar radius and distance from ring plane normalized to the radius of the resonator, R. Normalized propagation constant $\nu = 2\pi R / \lambda$ is also used, where λ is the vacuum wavelength. Azimuthal dipoles $\mathbf{P}_m = \hat{\varphi}_m \mathrm{P}_0 \exp(jl\varphi_m)$, $m = 1$, 2, …, q, are located evenly along the resonator circumference with $\rho = 1$ on the emitter plane ($\zeta = 0$), as illustrated in Fig. 1. All dipoles are assumed with a uniform moment of P_0 and a time dependence of $\exp(-j\omega t)$, $l = p - q$ is the topological Pancharatnam charge, p being the azimuthal order of the WGM involved and q the number of grating elements or dipoles. $\{\varphi_m = 2\pi m / q\}$ are the azimuthal angles of the dipoles. For all simulations in this work, $q = 36$ and $R = 3.9\,\mu$m are used, corresponding to one of the real devices demonstrated in Ref. [6].

If some point $Q(\rho, \varphi, \zeta)$ is located in the upper hemisphere ($\zeta > 0$, see Fig. 1), the field results from the interference among the radiation of all dipoles [7]:

$$\mathbf{E}_l(\rho,\varphi,\zeta) = \frac{\mathrm{A}}{R^3}\sum_{m=1}^{q}\exp(j\nu r_m)\exp(jl\varphi_m) \times\left[\left(\frac{\nu^2}{r_m}-j\frac{\nu}{r_m^2}-\frac{1}{r_m^3}\right)(\hat{r}_m\times\hat{\varphi}_m)\times\hat{r}_m-\left(j\frac{2\nu}{r_m^2}+\frac{2}{r_m^3}\right)(\hat{r}_m\cdot\hat{\varphi}_m)\cdot\hat{r}_m\right] \quad (1)$$

where $\mathrm{A} = \mathrm{P}_0 / (4\pi\varepsilon_0)$, r_m is the distance between Q and the mth dipole point $P_m(1, \varphi_m, 0)$, and $\hat{r}_m$ is the unit vector in the direction of P_mQ, pointing from P_m.

First, at a near-zone plane ($\zeta \ll \lambda / R$ or $\zeta \sim \lambda / R$), the terms of near-field ($1 / r^3$ decay) and middle-field ($1 / r^2$ decay) prevail, thus making the interference between adjacent dipoles dominant. Based on Eq. (1), Fig. 2(a) and 2(b) present the calculated normalized-intensity of the azimuthal and non-azimuthal components of the emission at $\zeta = 0.4\lambda / R$ when $l = 0$, suggesting that the SOP of the near-zone emission is

predominantly azimuthal. Alternatively, transverse components can be decomposed into E_x and E_y in Cartesian coordinates, as shown in Figs. 2(c) and 2(d), and these near-zone SOP patterns have been verified by the experiments (see Figs. 2(b) and 2(d) in Ref. [6]). Yet it is noteworthy that even in this near-zone some azimuthally polarized concentric ring patterns appear near the origin (Fig. 2(a)), indicating the emergence of far-field patterns.

On the other hand, in the far zone ($\zeta \gg \lambda / R$), the field mainly results from the interference of far-field radiation of all dipoles, and the near-zone terms (~$1 / r^2$ and ~$1 / r^3$) are neglected. Using the Fresnel diffraction approximation in the paraxial limit, the radial component of the vector field can be derived as:

$$E_{\rho,l}(\rho,\varphi,\zeta) = \mathbf{E}_l(\rho,\varphi,\zeta)\cdot\hat{\rho} = -\frac{\mathrm{A}}{R^3}\frac{\nu^2}{\zeta}\Phi(\rho,\zeta) \times\sum_{m=1}^{q}\exp(-j\nu\tan\Theta\cos\Delta\varphi_m)\exp(jl\varphi_m)\sin\Delta\varphi_m \quad (2)$$

where $\Phi(\rho,\zeta) = \exp\{j\nu[\zeta + (\rho^2 + 1) / 2\zeta]\}$ is the propagation phase factor, $\Theta = \tan^{-1}(\rho / \zeta)$ is the diffraction angle, and $\Delta\varphi_m = \varphi_m - \varphi$ is the azimuthal angle difference between Q and grating element m. By taking an approximate integral representation of the Bessel function of the first kind ($2\pi / q \ll 1$)

$$\sum_{m=1}^{q}\exp(-j\nu\tan\Theta\cos\Delta\varphi_m)\exp(jn\Delta\varphi_m) \approx j^n q J_n \quad (3)$$

and with the relation $J_{n-1}(x) + J_{n+1}(x) = (2n / x)\, J_n(x)$, we obtain the analytical expression for the far-field radial component

$$E_{\rho,l}(\rho,\varphi,\zeta) = j^l\frac{\mathrm{A}lq}{R^3}\frac{\nu}{\rho}\Phi(\rho,\zeta)\exp(jl\varphi)J_l \quad (4a)$$

where $J_l = J_l(-\nu\tan\Theta)$. Taking a similar process as above and with the relation $J_{n-1}(x) - J_{n+1}(x) = 2dJ_n(x) / dx$, we have the other field components as

$$E_{\varphi,l}(\rho,\varphi,\zeta) = j^{l-1}\frac{\mathrm{A}q}{R^3}\frac{\nu^2}{\zeta}\Phi(\rho,\zeta)\exp(jl\varphi)J_l' \quad (4b)$$

$$E_{\zeta,l}(\rho,\varphi,\zeta) = -j^l\frac{\mathrm{A}lq}{R^3}\frac{\nu}{\zeta}\Phi(\rho,\zeta)\exp(jl\varphi)J_l \quad (4c)$$

Eqs. (4a)-(4c) present a set of orthogonal cylindrical vector Bessel (CVB) modes for each of the cylindrical components. In Ref. [8], Hall has proven that the vector paraxial wave equation (PWE) has a family of Bessel-Gauss beam solutions. Here we demonstrate that the novel integrated OV beam emitters produce another class of Bessel beams, which shall be admitted by the vector PWE automatically, since the radiation of each single dipole element satisfies the wave equation. In other words, this CVB beam can be regarded as a special case of the diffraction integral theory for azimuthally polarized beam perturbed by circularly symmetric disturbance [9], and the disturbance in our case can be modeled as $P(r)E_\varphi(r,0) = \delta(r - R)\exp(jl\varphi)$ (see Eq. (12) in Ref. [9]), where $\delta(x)$ is the delta function.

These CVB modes possess several interesting features. Firstly, all components have the amplitudes proportional to the lth-order Bessel function of the first kind or to its first derivative:

$$\left|E_{\rho,l}\right|,\ \left|E_{\zeta,l}\right| \propto J_l(-\nu\tan\Theta),\ \left|E_{\varphi,l}\right| \propto J_l'(-\nu\tan\Theta) \quad (5)$$

therefore all orders of diffraction propagate in constant angles $\Theta_i^l = \tan^{-1}(-\chi_i^l / \nu)$ to the ζ axis, where χ_i^l is the ith extreme point of J_l (J_l' for $E_{\varphi,l}$). Fig. 3 shows the normalized intensity distribution of all field components as a function of Θ in different l orders. The order of the Bessel function, l, is an arbitrary charge, and can be adjusted by tuning the wavelength of the injected light [6].

Then, note that the amplitudes of the radial and longitudinal components are also proportional to l, thus these two components will not exist when $l = 0$, making the emitted beam purely azimuthal-polarized in the far field:

$$E_{\varphi,0}(\rho,\zeta) = j\frac{\mathrm{A}q}{R^3}\frac{\nu^2}{\zeta}\Phi(\rho,\zeta)J_1 \quad (6)$$

Cylindrical vector (CV) beams with pure azimuthal or radial polarization have been widely studied for their interesting properties and potential applications, and various methods have been proposed to generate CV beams [10]. Eq. (6) suggests that the angular grating-based OV beam emitter is a potential purely-polarized CV beam emitter as well. It is also worth to mention that, in contrast with scalar vortex beams, the CVB beam is characterized by the existence of an on-axis intensity null when $l = 0$ [11], as illustrated in Fig. 3(a). This null results from a polarization singularity, where the direction of the electric vector of the locally linear-polarized field is undefined, and this is also referred to as a V point in singular optics [12].

Above all, although each cylindrical component has a phase difference of $\pi / 2$ or π to others, all of them have an azimuthal phase dependence of $\exp(jl\varphi)$ (see Fig. 4), which identifies the OAM carried by this CVB beam [1]. In Ref. [6], Cai *et al.* have been able to experimentally measure the charge l, and here the complete theoretical expression is given. The Jones vector of the transverse field is

$$\mathbf{E}_{T,l} = \begin{bmatrix}E_{x,l}\\E_{y,l}\end{bmatrix} = -j^l\frac{\mathrm{A}q}{R^3}\frac{\nu^2}{2\zeta}\Phi(\rho,\zeta) \times\left\{J_{l-1}\exp\left[j(l-1)\varphi\right]\begin{bmatrix}1\\j\end{bmatrix} + J_{l+1}\exp\left[j(l+1)\varphi\right]\begin{bmatrix}1\\-j\end{bmatrix}\right\} \quad (7)$$

This indicates that the radiated CVB beam can be described as the superposition of two orthogonal scalar waves: a left hand circularly polarized (LHCP) beam with topological charge of $l - 1$ and a right hand circularly polarized (RHCP) beam with $l + 1$ [6]. As a result, $l - 1$ and $l + 1$ spiral arms are produced

when the emitted vortex is interfered with LHCP and RHCP Gaussian reference beams respectively (see Fig. 3 in Ref. [6]). It should be noted that for l = +1, the transverse field consists of a scalar wave with charge 0 and a wave with charge +2, and the wave with 0 charge causes the bright center (see Fig. 3(b)). For l = –1, the on-axis intensity is non-zero for the same reason. Besides, for l = 0, the CV beam in Eq. (6) is decomposed into two circularly polarized beams of opposite topological charge (–1 and +1); interpreted with the higher-order Poincaré sphere proposed by Milione *et al.*, these two components are exactly the polar basis of a l = 1 sphere, and the l = 0 beam of Eq. (6) locates on the equatorial point of (π, 0) [13].

In summary, using a model built on a simple dipole representation of grating scattering, we have derived the near- and far-zone emission characteristics of a novel angular grating-based OV beam emitters that agree well with the experimental results. Analytical expressions for the far-field paraxial beam have been obtained that reveal the emission as a class of CVB beams with tunable OAM, and predict the device as a potential pure CV beam emitter.

References

1. L. Allen, M. Beijersbergen, R. Spreeuw, and J. Woerdman, Phys. Rev. A **45**, 8185-8189 (1992).
2. G. Molina-Terriza, J. P. Torres, and L. Torner, Nat. Phys. **3**, 305-310 (2007).
3. M. W. Beijersbergen, R. Coerwinkel, M. Kristensen, and J. P. Woerdman, Opt. Commun. **112**, 321–327 (1994).
4. N. R. Heckenberg, R. McDuff, C. P. Smith, and A. White, Opt. Lett. **17**, 221–223 (1992).
5. C. R. Doerr and L. L. Buhl, Opt. Lett. **36**, 1209-1211 (2011).
6. X. Cai, J. Wang, M. J. Strain, B. Johnson-Morris, J. Zhu, M. Sorel, J. L. O'Brien, M. G. Thompson, and S. Yu, Science **338**, 363-366 (2012).
7. A. R. Von Hippel, *Dielectrics and Waves* (Wiley, 1954).
8. D. G. Hall, Opt. Lett. **21**, 9-11 (1996).
9. P. L. Greene and D. G. Hall, J. Opt. Soc. Am. A **13**, 962-966 (1996).
10. Q. Zhan, Adv. Opt. Photon. **1**, 1 (2009).
11. M. Padgett, J. Courtial, and L. Allen, Phys. Today **57**, 35-40 (2004).
12. I. Freund, Opt. Commun. **201**, 251-270 (2002).
13. G. Milione, H. I. Sztul, D. A. Nolan, and R. R. Alfano, Phys. Rev. Lett. **107**, 53601 (2011).

Figures

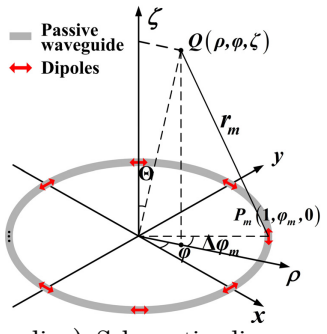

Fig. 1. (Color online) Schematic diagram of the dipole-model in the normalized cylindrical coordinate for interference analysis.

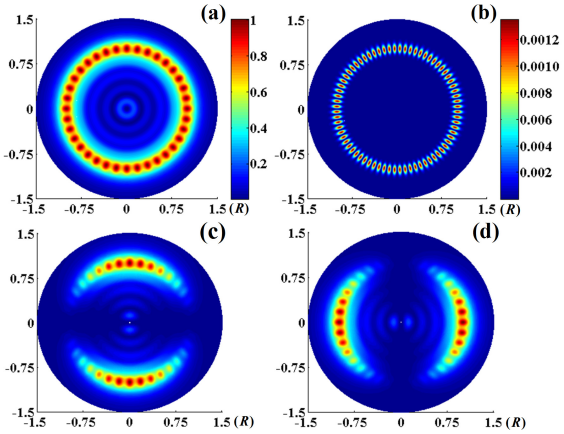

Fig. 2. (Color online) Simulated near-zone intensity distribution of different components at $\zeta = 0.4\lambda / R$ with l = 0: (a) E_φ, (b) E_ρ and E_ζ, (c) E_x, (d) E_y.

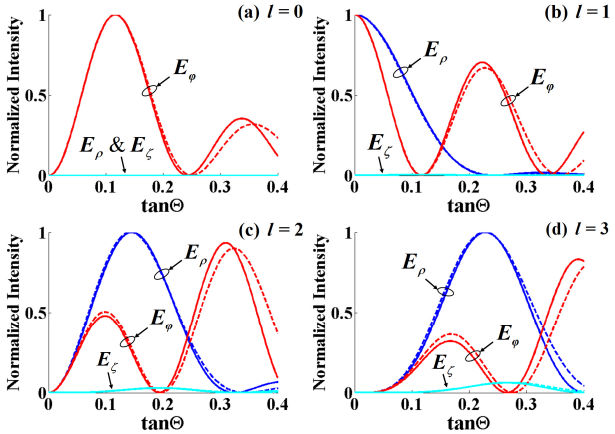

Fig. 3. (Color online) Calculated cross sections of the far-field intensity distribution of E_φ (red curves), E_ρ (blue curves), and E_ζ (green curves) as a function of diffraction angle Θ, with charges: (a) l = 0, (b) l = 1, (c) l = 2, (d) l = 3. Paraxial approximated results are presented (solid curves) as well as the nonparaxial ones (dashed curves).

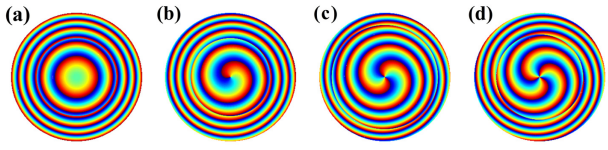

Fig. 4. (Color online) Calculated transversal phase distribution of the far-field (a) $E_\varphi(l = 0)$, (b) $E_\rho(l = 1)$, (c) E_ρ (l = 2), (d) $E_\varphi(l = 3)$.

Full citation listings:

1. L. Allen, M. Beijersbergen, R. Spreeuw, and J. Woerdman, "Orbital angular momentum of light and the transformation of Laguerre-Gaussian laser modes," Phys. Rev. A **45**, 8185-8189 (1992).
2. G. Molina-Terriza, J. P. Torres, and L. Torner, "Twisted photons," Nat. Phys. **3**, 305-310 (2007).
3. M. W. Beijersbergen, R. Coerwinkel, M. Kristensen, and J. P. Woerdman, "Helical-wavefront laser beams produced with a spiral phaseplate," Opt. Commun. **112**, 321–327 (1994).
4. N. R. Heckenberg, R. McDuff, C. P. Smith, and A. White, "Generation of optical phase singularities by computer-generated holograms," Opt. Lett. **17**, 221–223 (1992).
5. C. R. Doerr and L. L. Buhl, "Circular grating coupler for creating focused azimuthally and radially polarized beams," Opt. Lett. **36**, 1209-1211 (2011).
6. X. Cai, J. Wang, M. J. Strain, B. Johnson-Morris, J. Zhu, M. Sorel, J. L. O'Brien, M. G. Thompson, and S. Yu, "Integrated Compact Optical Vortex Beam Emitters," Science **338**, 363-366 (2012).
7. A. R. Von Hippel, *Dielectrics and Waves* (Wiley, 1954).
8. D. G. Hall, "Vector-beam solutions of Maxwell's wave equation," Opt. Lett. **21**, 9-11 (1996).
9. P. L. Greene and D. G. Hall, "Diffraction characteristics of the azimuthal Bessel–Gauss beam," J. Opt. Soc. Am. A **13**, 962-966 (1996).
10. Q. Zhan, "Cylindrical vector beams: from mathematical concepts to applications," Adv. Opt. Photon. **1**, 1 (2009).
11. M. Padgett, J. Courtial, and L. Allen, "Light's Orbital Angular Momentum," Phys. Today **57**, 35-40 (2004).
12. I. Freund, "Polarization singularity indices in Gaussian laser beams," Opt. Commun. **201**, 251-270 (2002).
13. G. Milione, H. I. Sztul, D. A. Nolan, and R. R. Alfano, "Higher-Order Poincaré Sphere, Stokes Parameters, and the Angular Momentum of Light," Phys. Rev. Lett. **107**, 53601 (2011).